IN SITU STRESS EVOLUTION DURING GROWTH OF TRANSITION METAL NITRIDE FILMS AND NANOCOMPOSITES

G. Abadias[1,*], L.E. Koutsokeras[1,2], P.A. Patsalas[2], W. Leroy[3], D. Depla[3]
S.V. Zlotsi[4], V.V. Uglov[4]

1 Institut P', Dpt. Physique et Mécanique des Matériaux, Université de Poitiers-CNRS-ENSMA, 86962 Chasseneuil-Futuroscope, France
2 Department of Materials Science and Engineering, University of Ioannina, 45110 Ioannina, Greece
3 Department of Solid State Sciences, Ghent University, Krijgslaan 281 (S1), 9000 Ghent, Belgium
4 Belarussian State University, Nezaleznastia av. 4, 220030 Minsk, Belarus

ABSTRACT

The issue of stress evolution during growth of hard transition metal nitride (TMN) based coatings is of vital importance to understand origin of intrinsic stress development and to control stress level in order to avoid mechanical failure of coated components and devices. By using *in situ* and real-time wafer curvature measurements based on a multiple-beam optical stress sensor (MOSS), basic insights on the atomistic mechanisms at the origin of stress development and stress relaxation can be obtained. In the present paper, a review of recent advances on stress development during reactive magnetron sputter-deposition of binary TMN films (TiN, ZrN, TaN) as wells as ternary systems (TiZrN, TiTaN) will be presented. The influence of growth energetics on the build-up of compressive stress will be addressed. A correlation between stress, texture and film morphology is demonstrated. Finally, illustration will be given for quaternary TiZrAlN nanocomposites.

Key words: multiple-beam optical stress sensor, thin film growth, grain boundary, defects, intrinsic stress, thermal stress, TiN, ZrN, TiTaN, Ti-Zr-Al-N

INTRODUCTION

Transition metal nitride (TMN) have been extensively studied in the last decades, owing to their excellent performance as hard, wear- and corrosion resistant coatings [1-3], but also as suitable template layers for group-III-nitride wide band-gap semiconductors [4,5], and recently as reflecting back contacts in solar cells [6,7]. Efforts have been made to further enhance their performance by designing ternary or multinary TMN systems [8-11], which offer the possibility of fine tuning the mechanical and/or electrical properties by adjusting the chemical composition with different metal or non-metal alloying elements.

---

* e-mail: gregory.abadias@univ-poitiers.fr, tel: (+33)549496748

These coatings are usually deposited by means of physical vapor deposition (PVD) techniques, which offer a better flexibility and control over growth process compared to chemical vapor deposition.

As PVD is a far-from equilibrium process, the film microstructure and morphology are kinetically controlled [12]. Growth kinetics and energetics play also a significant role in the formation of metastable phases, as for the stabilization of metastable $Ti_{1-x}Zr_xN$ and $Ti_{1-y}Ta_yN$ solid solutions of rocksalt structure by magnetron sputter-deposition [10]. However, as the film is rigidly attached to its substrate, any microstructural modification in the *growing layer* (e.g., formation of grain boundaries, introduction of dislocation, phase transformation, incorporation of defects/impurities) will lead to the development of growth (intrinsic) stress. Stress can also arise from strained regions at the *film/substrate interface* (lattice mismatch, difference in thermal expansion coefficient, intermixing) or changes at the *film/vacuum interface* (surface stress, adsorption of foreign species).

Stress in polycrystalline films depends intimately on the nucleation and growth conditions as well as on adatom mobility [13-15]. At low pressure, TMN films grown by PVD are generally under large compressive stresses [16]. This is due to their refractory character and the stabilization of point or cluster defects introduced in these growing layer by energetic incoming species, a mechanism known as 'atomic peening' [17]. However, there exists a subtle interplay between stress and microstructure in polycrystalline films [18], leading to stress evolution or stress reversal with film thickness. Consequently, TMN may exhibit stress gradients along their film thickness. In order to avoid excessive stress levels and mechanical failure of TMN-coated devices, stress needs to be carefully controlled. It is therefore of vital importance to understand the origin of stress build-up during thin film growth.

In situ and real-time wafer curvature technique offers a unique opportunity to measure with sub-monolayer sensitivity stress evolution during thin film deposition. As the film stress is continuously determined as a function of deposition time, the existence of stress gradients along the film thickness can be unambiguously evidenced, even down to a nanometer scale where conventional X-ray diffraction (XRD) techniques fail [19].

Using a multiple-beam optical stress sensor (MOSS) implemented in a vacuum chamber, the presence of stress gradients in ~100 nm thick magnetron-sputtered TiN films could be revealed for the first time [20]: the stress was found to be largely compressive (~−5 GPa) close to the film/substrate interface, while the measured stress decreased to ~−0.8 GPa at 100 nm thickness. These *in situ* results are in good agreement with data previously reported by Köstenbauer *et al.* [21] and Machunze *et al.* [22] from *ex situ* wafer curvature experiments, although the stress-gradients were measured over ~2 μm thick TiN films.

In the present paper, the stress evolution during reactive magnetron sputter-deposition of various TMN films is investigated using MOSS. A detailed survey of the influence of main deposition parameters (Ar working pressure, substrate bias voltage, N_2 flow rate) is provided for TiN films. The stress behavior in TiN films is then compared with other binary TMN, namely ZrN and TaN, as well as ternary $Ti_{1-x}Zr_xN$ and $Ti_{1-y}Ta_yN$ films. Basic mechanisms at the origin of stress development are proposed, based on the contribution of particle flux and energy flux. A close correlation between film microstructure, growth morphology and preferred orientation is demonstrated. Finally, the case study of quaternary TiZrAlN films, which exhibit a microstructural transition from single-phase metastable solid solutions towards bi-phase nanocomposites at Al content higher than 5 at.%, is presented.

EXPERIMENTAL PROCEDURE

Binary TiN, ZrN and TaN films were deposited at T_s=300°C on Si (001) wafers using dc reactive unbalanced magnetron sputtering (MS) from Ti (99.995% purity), Zr (99.2% purity) and Ta (99.998% purity) targets, respectively. The three metal targets were 7.5-cm-diameter water-cooled planar magnetron sources, arranged on a confocal magnetron cluster, and located at a distance of 18 cm from the substrate, which was mounted on a rotating sample holder coupled with a heating element. Prior to deposition, the vacuum chamber was pumped with a cryogenic pump down to $\sim 2\times 10^{-6}$ Pa, while an Ar+N_2 gas mixture was introduced during reactive sputtering. To change the energy of the incoming species (sputtered atoms, backscattered neutrals, ions) the Ar pressure, substrate bias voltage and configuration of magnetrons (balanced/unbalanced mode) were changed. Ternary $Ti_{1-x}Zr_xN$ and $Ti_{1-y}Ta_yN$ films were also synthesized by co-sputtering of Ti+Zr or Ti+Ta targets in Ar+N_2 atmosphere. The x (y) atomic fraction was varied by changing the respective target powers.

Another series of magnetron sputter-deposited TiN films was performed in a different vacuum chamber equipped with a highly unbalanced 5-cm diameter planar magnetron Ti (99.97% purity) target, located at 13 cm from the substrate, in order to study the influence of particle and energy flux on the stress and preferred orientation development. No intentional heating of the substrate was employed for this series and all the deposition parameters, except the angle of incidence of the incoming flux, were kept similar to the previous work of Mahieu *et al*. for which the energy and particle fluxes towards the substrate were carefully determined [23].

Stress evolution in the film was monitored in real time during growth using a multi-beam optical stress sensor (MOSS) technique [24] designed by kSA and implemented in the sputtering system. A schematic illustration of the experimental set-up is shown in *fig. 1*.
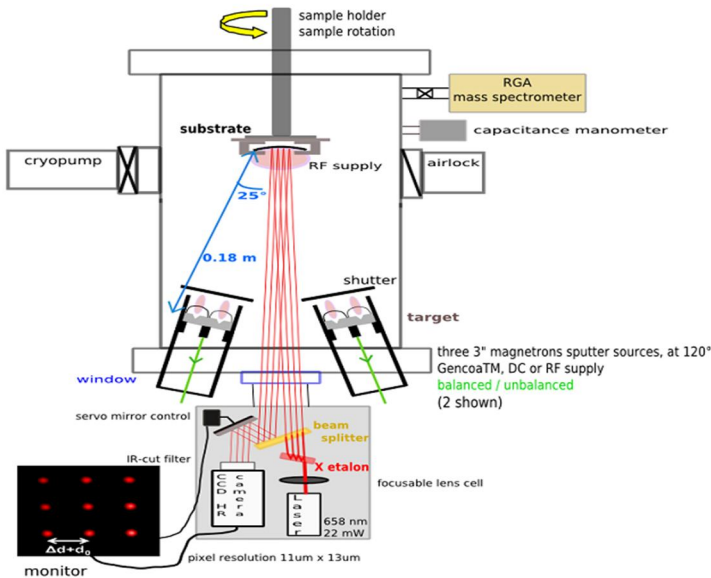
Fig. 1 – Schematic of the in situ MOSS implemented in the magnetron sputter-deposition chamber

The measurement is based on the determination of the substrate curvature κ and lays on the deflection of a 2D array of parallel laser beams (created using highly reflective X and Y etalons) from the bended substrate. The reflected beams are recorded on a high resolution charge-coupled device (CCD) camera with a typical acquisition time of 0.2 s. Changes in substrate curvature due to an evolving stress in the film produce changes in the angular divergence of the beam array, and therefore changes in the spacing between adjacent laser spots on the CCD camera. The Si substrates, with thickness $h_s = 210 \pm 5\mu m$, are mounted on a specially designed holder to allow unconstrained bending of the substrate. The intrinsic force per unit width, F/w, given by the product between the average stress $<\sigma>$ and film thickness h, is calculated from the change in curvature $\Delta\kappa$ using the well-known Stoney equation [25], $F/w = <\sigma>.h = 1/6\,(Y_s h_s^2 \Delta\kappa)$, where Y_s is the biaxial modulus of the substrate taken equal to 180.5 GPa for (001) single crystal Si wafer [26]. In a graph of F/w versus h, the instantaneous stress, σ, is obtained from the slope d(F/w)/dh and corresponds to the contribution of a newly deposited layer on the film surface and/or any stress evolution occurring in the already-grown film. By convention, positive σ values refer to a tensile stress state.

The surface morphology of the films was characterized by Atomic Force Microscopy (AFM) using a Multimode Digital Instrument device operating in

tapping mode, while film cross-sectional sample views were imaged by scanning electron microscopy (SEM) using a JEOL JSM 7000F equipped with a field emission gun. The crystallographic orientation was determined from x-ray diffraction (XRD) patterns recorded on a D8 Bruker diffractometer using Cu Kα radiation and operating in θ–2θ Bragg-Brentano configuration. Energy dispersive X-ray spectroscopy (EDX) was used to determine the metallic content of TMN, while Rutherford backscattering spectroscopy (RBS) experiments were carried out to quantify the N content [10].

RESULTS AND DISCUSSION

Binary TMN films. *Fig. 2a* shows the evolution of F/w for TiN, ZrN and TaN films deposited by reactive MS at relatively low Ar pressure (<0.32 Pa) and low N_2 flow rate (see Ref. 10 for more details), for a target-to-substrate distance of d_{T-S}=18 cm. The magnetrons were slightly unbalanced for the Ti and Zr target, and balanced for the Ta one. One can see that large compressive stress initially develops, the instantaneous stress reaching ~–5 GPa for h<20 nm. With increasing film thickness, different stress evolutions are evidenced depending on the type of binary TMN film. While a steady stress state is noticed for TaN, a slight decrease of compressive stress is found for ZrN; the TiN film exhibits a pronounced non-uniform stress variation over its thickness. For this latter, the instantaneous stress even becomes tensile (+0.16 GPa) beyond 50-70 nm. These results reflect the competition between different stress sources: compressive stress due to atomic peening [15, 17] and tensile stress due to attractive forces at grain boundary [20, 27]. We will show in the following that the difference in stress evolutions between the three investigated TMN films is related to the different growth energetics, also at the origin of different microstructural and morphological growth evolution with increasing film thickness.

Fig. 2b shows the stress evolution after growth interrupt for TiN films deposited at T_s=300°C (series #1) and RT (series #2): while for the first series no stress evolution is noticed when the deposition is stopped, a significant stress evolution towards tensile direction is noticed for the second series. Moreover, it is interesting to see that this evolution is reversible when the plasma is switched on again, ruling out implicitly any stress relaxation in the buried layers. The stress relaxation mechanism due to flow of excess adatoms from grain boundary towards the surface, proposed by Chason et al. [28] for high-mobility metals, is unlikely to operate for refractory compounds like TiN (T_s/T_m<0.18, where T_s= substrate temperature and T_m=3222 K is the melting temperature). In fact, the observed difference is due to contribution of thermal stress: for the first series, the substrate temperature is fixed at T_s=300°C, while for the second series, no intentional heating of the substrate was used. However, the plasma discharge causes an unavoidable temperature rise in the film, and consequently

a variation in thermal stress due to the difference in thermal expansion coefficients between the TiN film ($\alpha_f = 9.35 \ 10^{-6} \ K^{-1}$) and Si substrate ($\alpha_s = 3.1 \ 10^{-6} \ K^{-1}$). A passive thermal probe was used to determine the energy flux and substrate temperature for films of series #2. The temperature rise during deposition reached 120 to 165°C, depending on the N_2 flux used. The calculated thermal stress was in good agreement with the experimental data. This result points out the importance of employing *in situ* experiments to reveal possible stress modification during growth interruption. In the present case, the contribution of intrinsic (growth) stress can only be obtained after thermal stress subtraction for TiN films of series #2.
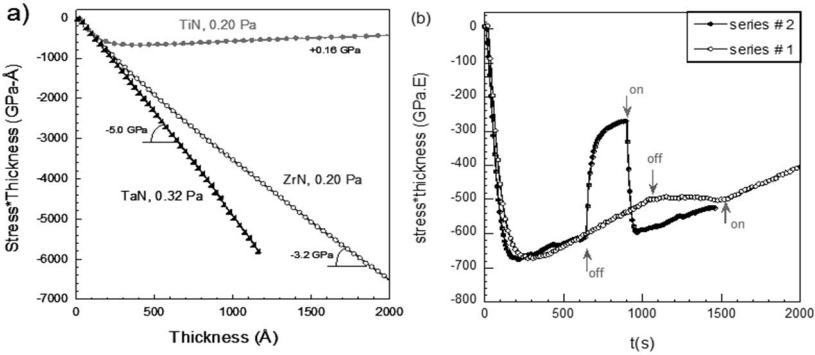

Fig. 2 – a) Evolution of the stress*thickness product (F/w) during reactive MS of TiN, ZrN and TaN films [29]. b) Stress evolution during growth interrupts for two different series of TiN films

Figure 3 shows the influence of process parameters, such as Ar working pressure, substrate bias voltage and magnetron configuration on the stress evolutions of TiN, ZrN and TaN films. Each of these parameters affect the total energy flux deposited towards the growing film: an increase in Ar pressure leads to a larger number of collisions in the gas phase, Ar ions gain energy when a bias voltage is applied to the substrate and a larger fraction of ionized Ar species is obtained when the magnetic field extends further towards the substrate. Note also that the energy of the incoming species (sputtered atoms and backscattered Ar) increases with increasing mass target (i.e. from Ti to Zr and Ta), as deduced from SRIM calculations [29].

The stress data shown in fig.3 show that larger compressive stress develops in TMN films when
- the mass density of the transition metal increases (fixed Ar pressure)
- the Ar working pressure is reduced
- the bias voltage is increased
- the magnetron configuration is unbalanced

All these observations support the scenario that compressive stress is due to the incorporation of growth-induced defects [30, 31], as a consequence of the incoming flux of energetic particles with typical energy exceeding the subplantation threshold [29, 32].
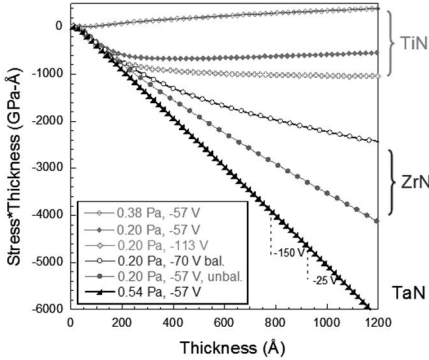

Fig. 3 – Influence of MS process parameter (Ar pressure, substrate bias voltage and magnetron configuration) on the stress evolution of TiN, ZrN and TaN films [29]

Ternary TMN films. *Figure 4* shows the stress evolution as a function of Ta content of $Ti_{1-y}Ta_yN$ films deposited at 0.31 Pa. With increasing Ta content, the stress becomes more compressive; this is accompanied by a change in growth morphology from (111)-textured columns with 'zone-T' type [12, 23] for $y<0.5$ to (002)-oriented fine 'globular' grains for $y>0.5$ This change in film microstructure is also reflected by the difference in top surface morphology, as revealed from AFM images (*fig.5b*). Similar 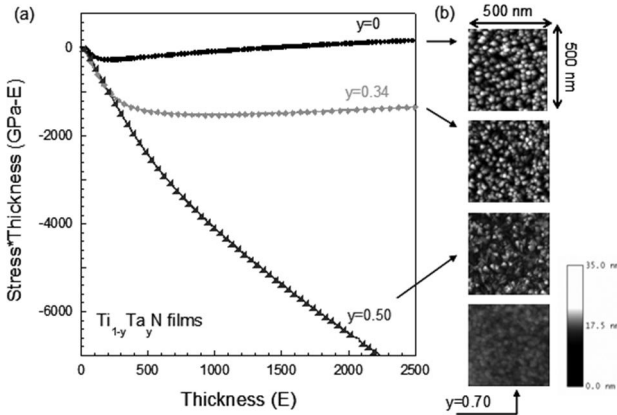effects, though less pronounced, are observed for $Ti_{1-x}Zr_xN$ films [10, 29]. In particular, TiN-rich films exhibit a rough surface morphology due to the emergence of facetted columns , while the surface of TaN-rich films is smooth and featureless.

These results show a clear correlation between stress and microstructure evolution during growth of ternary TMN films.

Fig. 4 – a) Evolution of the stress*thickness product (F/w) during reactive MS ternary $Ti_{1-y}Ta_yN$ films at 0.31 Pa. b) Evolution of AFM surface topography (500 nm × 500 nm) of 300 nm thick films with Ta content, y
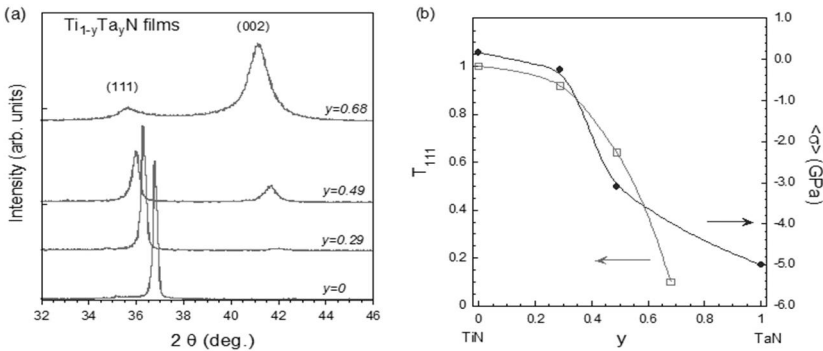
Fig. 5 – a) XRD patterns of $Ti_{1-y}Ta_yN$ films (300 nm thick) deposited at 0.31 Pa.
b) Evolution of (111) texture coefficient (T_{111}) and biaxial stress ($<\sigma>$) of 300 nm thick
films with Ta content, y

Both variations can be rationalized by considering the increase of growth energetics with increasing Ta (or Zr) content: the higher energetic conditions of the deposition inhibit the columnar growth due the creation and destruction of nucleation sites, and favors the growth of thermodynamically more stable (002) planes ($\gamma_{002}<\gamma_{111}$ for TMN with rocksalt structure, where γ is the surface energy). The change in film preferred orientation is evidenced from XRD patterns (see fig.5a). A clear correlation between biaxial stress level and (111) texture coefficient is also found (*fig.5b*).

Quaternary TMN films. In order to further improve the thermal stability as well as oxidation and corrosion resistance of TiN coatings, Al is often used as an alloying element. Indeed, TiN starts to oxidize rapidly at about 500°C and forms the rutile structure TiO_2, which lead to deteriorating mechanical properties. The use of $Ti_{1-x}Al_xN$ coatings [33] significantly improves the cutting and machining performance of tools, even up to temperature of 900°C, due to the formation of a protective Al-rich oxide layer at the film surface. This motivated the synthesis of quaternary TiZrAlN films by reactive MS in the present study. Preliminary results on the structure of as-grown films has been reported in Ref. 34. The evolution of XRD patterns of TiZrAlN films with Al content in the range 0-10.5% is shown in fig.6a. A transition from metastable solid solutions with rocksalt structure and (111) texture towards a nanocomposite structure is evidenced at ~5 at.% Al

Fig.6b shows the stress evolution of quaternary alloys with Al content in the range 0-10.5 at.%. Large stress variations are observed with increasing Al content. Interestingly, the addition of Al into the TiZrN lattice leads to the development of a large, steady-state compressive stress. This could be related to the incorporation of Al atoms in substitutional sites of the rocksalt structure of TiZrN and associated lattice distortion. Additional XRD experiments should be

carried to ascertain this statement. One can also see that a significant stress reduction accompanies the structural transition observed at 5.0 at. % Al: the formation of nanocomposites proceeds with a reduction of compressive stress. To the best of our knowledge, this is the first *in situ* and real-time stress measurements during deposition of hard nanocomposite films. Further experiments aiming at investigating the influence of grain boundary as preferable sites of defects annihilation would bring insights into the issue of stress development in nanoscale materials.
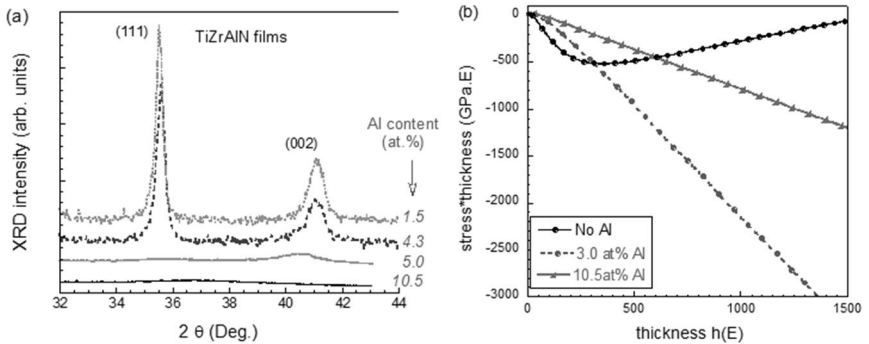

Fig. 6 – a) Evolution of XRD patterns of TiZrAlN films deposited at 0.19 Pa with Al content. b) *In situ* stress evolution during growth of selected quaternary films with 0, 3.0 and 10.5 at.% Al

CONCLUSIONS

Complex stress evolution during growth by reactive magnetron sputtering of TiN-based transition metal nitride films could be evidenced using *in situ* and real-time wafer curvature technique. The stress development in TMN films is the result of two kinetically competitive stress generation mechanisms: atomic peening induced compressive stress and inter-columnar attraction induced tensile stress. Stress evolutions were correlated with the energy of the impinging species, as estimated using SRIM calculations. At low energetic conditions, a competitive columnar growth (zone-T) is found with the presence of stress gradients (compression at the film/substrate interface and tension in the upper part of the film), typical of Ti-rich Ti-Zr-N films, correlated with the development of a (111) texture. At higher energetic deposition conditions, a dense 'globular'-like microstructure with smooth surface and uniform compressive stress over the whole thickness is observed, typical of Ta-rich Ti-Ta-N films. For the first time, *in situ* stress data are reported for TiN-based hard nanocomposite films.

REFERENCES

[1] J.E. Sundgren, Thin Solid Films, 1985, 128, P 21
[2] P. Hedenqvist , M. Olsson , P. Wallén et al. Surf. Coat. Tech., 1990, 41, P 243
[3] P. H. Mayrhofer, C.Mitterer, L.Hultman, H.Clemens, Progr.Mater.Sci., 2006, 51, P 1032
[4] G.M. Matenoglou, L.E. Koutsokeras, P. Patsalas, Appl. Phys. Lett., 2009, 94, P 152108
[5] T. Seppänen, L. Hultman, J. Birch, Appl. Phys. Lett., 2006, 89, P 181928
[6] S. Schleussner, T. Kubart, T. Törndahl, M. Edoff, Thin Solid Films, 2009, 517, P 5548
[7] S. Mahieu, W. P. Leroy, K. Van Aeken et al. Solar Energy, 2011, 85, P 538
[8] G. M. Matenoglou, L. E. Koutsokeras, Ch. E. Lekka et al., Surf. Coat. Tech., 2009, 204, P 911
[9] D.G. Sangiovanni, V. Chirita, L. Hultman, Phys. Rev. B, 2010, 81, P 104107
[10] G. Abadias, L. E. Koutsokeras, S. N. Dub et al., J. Vac. Sci. Tech. A, 2010, 28, P 541
[11] V. V. Uglov, V. M. Anishchik, S. V. Zlotski, G. Abadias, Surf. Coat. Tech., 2006, 200, P 6389
[12] S. Mahieu, P. Ghekiere, D. Depla, R. De Gryse, Thin Sold Films, 2006, 515, P 1229
[13] J.A. Floro, E. Chason, R.C. Cammarata, D.J. Srolovitz, MRS Bulletin, 2002, 27, P 19
[14] R. Koch, Surf. Coat. Technol., 2010, 204, P 1973
[15] H. Windischmann, Crit. Rev. Solid. State Phys., 1992, 17, P 547
[16] G. Abadias, Surf. Coat. Technol., 2008, 202, P 2223.
[17] F. M. d'Heurle, Metall. Trans., 1970, 1 P 725
[18] G. C. A. M. Janssen, Thin Solid Films, 2007, 515, P 6654.
[19] I. C. Noyan and J. B. Cohen, Residual Stress, Measurement by Diffraction and Interpretation, Springer-Verlag, New York, 1987
[20] G. Abadias, Ph. Guerin, Appl. Phys. Lett., 2008, 93, P 111908
[21] H. Köstenbauer, G.A.Fontalvo, M.Kapp et al., Surf.Coat.Tech., 2007, 201, P 4777
[22] R. Machunze, G. C. A. M Janssen, Surf. Coat. Technol., 2008, 203, P 550
[23] S. Mahieu, D. Depla, J. Phys. D : Appl. Phys., 2009, 42, P 053002
[24] J.A. Floro, E. Chason, S.R. Lee et al. J. Electron. Mater., 1997, 26, P 969
[25] G. Stoney, Proc. R. Soc. London A, 1909, 82, P 172
[26] G.C.A.M. Janssen, M.M. Abdalla, F. Van Keulen et al. Thin Solid Films, 2009, 517, P 1858
[27] W. D. Nix, B. M. Clemens, J. Mater. Res., 1999, 14, P 3467
[28] E. Chason, B.W. Sheldon, L. B. Freund, J.A. Floro, S.J. Hearne., Phys. Rev. Lett., 2002, 88, P 156103
[29] G. Abadias, L. E. Koutsokeras, Ph. Guerin, P. Patsalas, Thin Solid Films, 2009, 518, P 1532
[30] .J-D. Kamminga, Th. H. De Keijser, R. Delhez, E. J. Mittemeijer, J. Appl. Phys., 2000, 88, P 6332
[31] .G. Abadias, Y.Y. Tse, Ph. Guerin, V. Pelosin, J. Appl. Phys., 2006, 99, P 113519
[32] P. Patsalas, C. Gravalidis, S. Logothetidis, J. Appl. Phys., 2004, 96, P 6264
[33] S. Pal Dey, S.C. Deevi, Mat. Sci. Eng. A, 2003, 342, P 58
[34] G. Abadias, V.V. Uglov, S.V. Zlotski. Proc. of the Intern. Conf. Nanomeeting, 24-27 Mai 2011, Belarus, P 458